

An Equalizer Adaptation Algorithm to Reduce Jitter in Binary Receivers

Anthony Chan Carusone, *Member, IEEE*

Abstract—This brief describes a hardware-efficient technique for adaptive equalization that minimizes jitter in baseband binary nonreturn-to-zero serial links. Whereas traditional least mean square (LMS) adaptation minimizes the mean squared error only at the center of the received eye pattern, this algorithm explicitly includes low jitter as part of its optimization criteria. The resulting equalizer coefficients provide a compromise between maximizing noise margin and minimizing jitter at the equalizer output. The adaptation algorithm operates on 1-bit (signed) signals and can be efficiently combined with binary phase detection in an integrated receiver. Behavioral simulations for a 10-Gb/s optical fiber link show that the proposed approach improves timing margin compared with sign–sign LMS adaptation.

Index Terms—Adaptive equalization, adaptive filters, clock and data recovery, fiber optic communication, least mean square (LMS) algorithm.

I. INTRODUCTION

THIS brief presents a practical technique for the adaptation of equalizers to minimize jitter in baseband binary communication. Timing margin (horizontal eye opening) is often a more critical system parameter than noise margin (vertical eye opening) in serial links above 1 Gb/s. Therefore, an equalizer that minimizes jitter may be preferable to one optimized for maximum noise margin at center of the received eye. This is true, for example, in many chip-to-chip communication applications and fiber optic links.

Several techniques have recently been proposed to explicitly minimize jitter in binary receivers. In [1], a nonlinear analog circuit varies the receiver’s delay depending on the received bit sequence. Doing so eliminates pattern-dependent jitter arising from one bit-period of post-cursor intersymbol interference (ISI). No adaptation algorithm is proposed to optimize the amount of delay. In [2], the tap weights of a linear transmit equalizer are optimized to minimize the bit-error rate (BER) on a multigigabit per second chip-to-chip link. The effects of both transmitter and receiver jitter are included in the optimization. However, the optimization is performed off-line assuming *a priori* knowledge of the channel response and noise statistics. No adaptation algorithm is proposed to perform the optimization automatically during operation of the link. In [3], equalization is used to minimize pattern-dependent jitter over backplanes. The tap-weights of a baud-rate linear equalizer are chosen to force the equalized pulse response to satisfy the Nyquist-2 criteria. This results in zero pattern-dependent

Manuscript received August 26, 2005; revised March 2, 2006. This paper was recommended by Associate Editor F. C. M. Lau.

The author is with the Department of Electrical and Computer Engineering, University of Toronto, Toronto, ON L9H 4W4, Canada (e-mail: tcc@eecg.utoronto.ca).

Digital Object Identifier 10.1109/TCSII.2006.881161

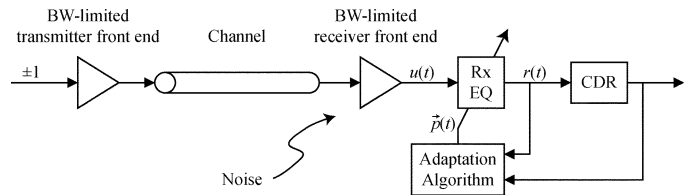


Fig. 1. System model for a binary link with adaptive equalization.

jitter, but does not treat noise and random jitter. Finally, the adaptation algorithm presented in [4] compromises between minimizing the mean squared error (MSE) at the center of the received eye and at its zero-crossings.

In this brief, first a new gradient descent adaptation algorithm is derived. The algorithm’s objective function takes into account both vertical and horizontal eye opening, as well as a term that prevents excessive tap weight drift. Then, signed versions of the state and error signals are used to reduce the adaptation algorithm’s complexity. Finally, a hardware-efficient implementation is suggested that combines the adaptive algorithm with a data-driven binary phase detector. The result is an adaptive equalizer that compromises between maximizing both vertical and horizontal eye openings simultaneously. Compared with a receiver implementing conventional sign–sign least mean squared (LMS) adaptation, the hardware overhead required is only simple digital logic. Simulation results for a 10-Gb/s fiber optic link indicate significant performance improvements using the proposed “signed jitter-reducing” adaptation algorithm, particularly when applied to a fractionally spaced equalizer.

II. ADAPTATION ALGORITHMS FOR BINARY EQUALIZERS

The system model employed in this work is shown in Fig. 1. It includes a bandwidth-limited binary nonreturn-to-zero (NRZ) transmitter, the channel, a bandwidth-limited receiver front end, and equalizer followed by a clock-and-data recovery system (CDR). The transmitted waveform $d(t)$ is bipolar with a bit period of T , $d(kT) = \pm 1$. A N -tap continuous-time finite-impulse response (FIR) equalizer with a tap spacing of τ is assumed (Fig. 2) similar to those described in, for instance, [5], [6] for data rates up to 30 Gb/s, although the adaptation algorithms derived are applicable to any adaptive linear combiner. The tap weights $\vec{p}(t) = [p_1(t) \ \cdots \ p_N(t)]^T$ are time varying under the control of an adaptation algorithm. The equalizer input is $u(t)$ and the equalizer output is $r(t) = \vec{p}^T(t)\vec{u}(t)$ where $\vec{u}(t) = [u(t) \ u(t - \tau) \ \cdots \ u(t - N\tau + \tau)]^T$.

Following the equalizer is a phase-locked loop with a data-driven binary (early–late) phase detector for clock recovery. For example, an Alexander phase detector [7] automatically retimes the data and has been successfully used at 10 Gb/s in CMOS integrated circuits [8].

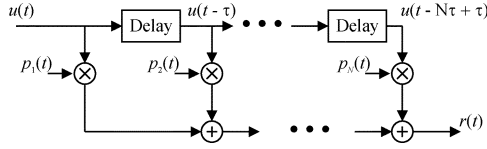


Fig. 2. Detailed block diagram of the FIR equalizer.

A. LMS Adaptation

Gradient descent optimization minimizes some objective function by iteratively updating parameters in a direction opposite the objective function's gradient. The traditional LMS algorithm is an approximate gradient descent optimizer. Its objective function is the mean squared error between the equalizer output and the desired equalizer output, here assumed to be the transmitted waveform $d(t)$, sampled at the center of the eye pattern.¹ Letting $e(kT) = d(kT) - r(kT)$, the mean squared error is

$$\xi = E [e^2(kT)]. \quad (1)$$

The approximation comes in using the instantaneous value of the squared error as a noisy estimate of its expected value. A constant μ is defined to control the adaptation's rate of convergence. The result is the familiar LMS update equation

$$\vec{p}(kT) = \vec{p}(kT - T) + 2\mu e(kT)\vec{u}(kT). \quad (2)$$

Hence, the LMS algorithm only minimizes the mean squared error at the sampling instants (i.e., at the center of the received eye pattern). It can therefore permit excessive jitter to persist even after convergence, as demonstrated later with simulations.

B. Jitter-Reducing Adaptation

One way to reduce jitter in the equalizer output is to include its mean squared error at zero-crossings

$$\zeta = E \left[e^2 \left(kT - \frac{T}{2} \right) \middle| d(kT) \neq d(kT - T) \right] \quad (3)$$

into the objective function being minimized. In (3), $E[x|Y]$ is the expected value of x when Y is true. Since the desired signal at the zero-crossings is $d(kT - T/2) = 0$, the error signal is simply $e(kT - T/2) = -r(kT - T/2)$. Note that jitter at the equalizer output is proportional to $\sqrt{\zeta}$, but inversely proportional to the slope of the equalizer output during transitions. Hence, low bandwidth or slow rise/fall-times at the equalizer output will make it more difficult to reduce jitter this way.

An additional measure is required to ensure the algorithm's robustness. It is well known that in fractionally spaced equalizers, there can be high correlation between neighboring tap signals, $u(t)$ and $u(t + \tau)$, causing the tap weights to drift using LMS adaptation to high absolute values [9]. These convergence problems are even more serious when signed LMS adaptation is used, as in the next section. Nevertheless, fractional tap spacing has the potential for better performance than symbol-spacing, particularly in the presence of circuit nonidealities. To avoid excessive tap-weight drift, an additional term may be added to

¹The delay through the channel and equalizer has been ignored here, without loss of generality.

the adaptation algorithm's objective function which favors small absolute values of the tap weights [10]. In this work, the squared sum of the tap weights is used

$$\varsigma = \vec{p}^T \vec{p}. \quad (4)$$

The objective function used for optimizing binary equalizers in this work is a weighted sum of (1), (3) and (4), $J_1 = a_1\xi + a_2\zeta + a_3\varsigma$. In order to fix the location of the main tap weight and provide a known nominal eye opening, one tap is adapted using a modified objective function for which the jitter (mean squared error at zero-crossings) is not included, $J_2 = a_1\xi + a_3\varsigma$.

As in the LMS algorithm, instantaneous values of the error signals may be used as noisy versions of their expected values to estimate the gradients of the objective functions

$$\frac{\partial J_1}{\partial \vec{p}} \approx -2a_1e(kT)\vec{u}(kT) - 2a_2r \left(kT - \frac{T}{2} \right) \vec{u} \left(kT - \frac{T}{2} \right) + 2a_3\vec{p}(kT) \quad (5)$$

$$\frac{\partial J_2}{\partial \vec{p}} \approx -2a_1e(kT)\vec{u}(kT) + 2a_3\vec{p}(kT). \quad (6)$$

These gradient estimates may then be used to perform an iterative approximate gradient descent optimization

$$\begin{aligned} \vec{p}(kT) = & \vec{p}(kT - T) + 2\mu [a_1e(kT)\vec{u}(kT) \\ & + \vec{w}(kT) \otimes a_2r \left(kT - \frac{T}{2} \right) \vec{u} \left(kT - \frac{T}{2} \right) \\ & - a_3\vec{p}(kT)] \end{aligned} \quad (7)$$

where \otimes denotes element-by-element vector multiplication and $\vec{w}(kT) = [w_1(kT) \ \dots \ w_N(kT)]^T$ is a binary vector that selectively disables the second of the three update terms between square brackets in (7). The term is disabled whenever there is no data transition in accordance with (6), and for the equalizer's "main" tap p_i as mentioned above. Hence,

$$w_j(kT) = \begin{cases} 0, & d(kT) = d(kT - T) \text{ or } j = i \\ 1, & \text{otherwise.} \end{cases} \quad (8)$$

The adaptation algorithm described in [4] is actually a special case of (7) and (8) for which $a_3 = 0$. That algorithm was arrived at heuristically whereas here it is derived as an approximate gradient descent optimizer for an objective function that balances noise margin, jitter, and robustness of convergence. Substituting $a_1 = 1$ and $a_2 = a_3 = 0$ into (7) yields the standard LMS update (2).

C. Signed Algorithms and Hardware Implementation

In practical receivers at 5+ Gb/s, often only one-bit (signed) quantities are used to simplify the multiply-accumulate operations in an adaptive algorithm [11]. This simplification can also be applied to jitter-reducing adaptation. Taking the sign of \vec{u} , r and e in (7) results in the simplified update equation

$$\begin{aligned} \vec{p}(kT) = & \vec{p}(kT - T) + 2\mu \left[a_1 \text{sgn}[e(kT)]\vec{u}(kT) \right. \\ & + \vec{w}(kT) \otimes a_2 \text{sgn} \left[r \left(kT - \frac{T}{2} \right) \vec{u} \left(kT - \frac{T}{2} \right) \right] \\ & \left. - a_3\vec{p}(kT) \right]. \end{aligned} \quad (9)$$

Equations (8) and (9) define "signed jitter-reducing adaptation." Using signed signals greatly simplifies an integrated circuit implementation of the adaptation algorithm. A block

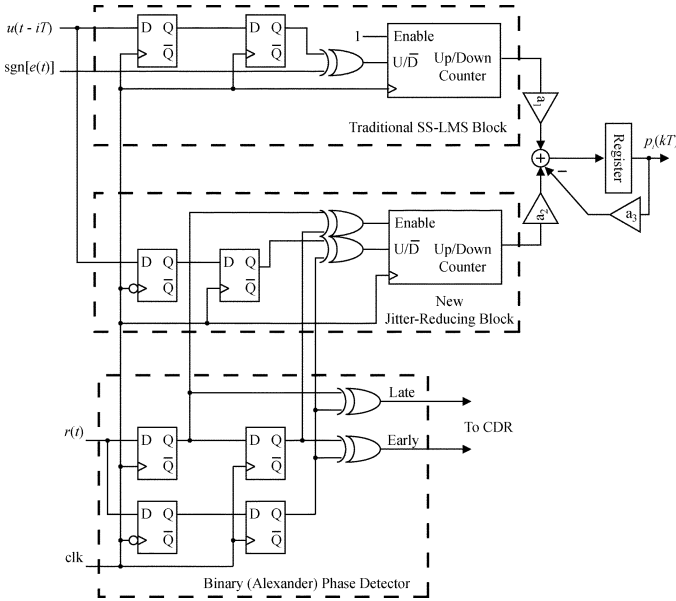


Fig. 3. Block diagram of a system implementing signed jitter-reducing adaptation. Only the components labeled “New Jitter-Reducing Block” represent additional hardware compared to traditional signed LMS adaptation.

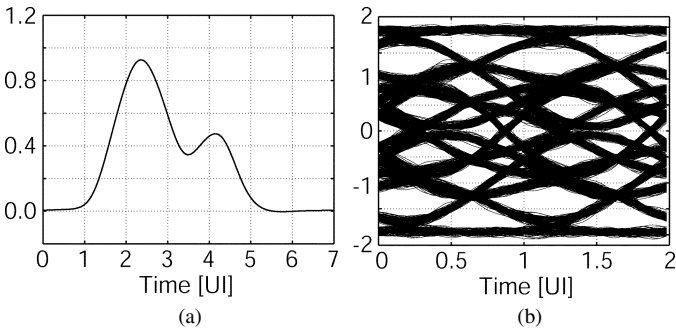


Fig. 4. Modeled channel response without equalization. (a) Pulse response. (b) Eye diagram.

diagram of a practical system implementing signed jitter-reducing adaptation is shown in Fig. 3. Notice that most of the digital signals required to iterate (9) are readily available in CDRs employing Alexander phase detection. One of the error signals in (9) $\text{sgn}[r(kT - T/2)]$ is also used by the CDR to perform early-late phase detection. Furthermore, the transition detector required to generate \vec{w} also appears in the CDR. Finally, the state signals $\text{sgn}[u]$ are also required by traditional signed LMS algorithms, although (9) requires them to be sampled twice per bit period instead of once. Fortunately, the clock phase required for the additional sampler is also required by the CDR. So, the additional hardware required to accommodate the jitter-reducing adaptation consists only of simple digital logic (flip-flops and XOR gates). Based on Fig. 3, the addition of the “new jitter-reducing block” would roughly double the hardware (and power) of the adaptation circuitry compared with traditional signed LMS adaptation. If the adaptation is only required to track relatively slow variations in the link due to temperature changes, aging, etc., all of the adaptation circuitry can be clocked at a much slower rate to save power.

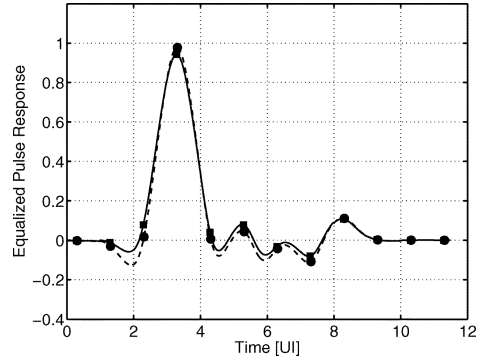


Fig. 5. Equalized pulse responses with a 5-tap baud rate equalizer adapted using the traditional sign–sign LMS algorithm (dashed line, circular markers) and the signed jitter-reducing adaptation algorithm (solid line, square markers).

III. SIMULATIONS

The remainder of the brief will compare the performance of signed jitter-reducing adaptation with traditional sign–sign LMS adaptation for a typical application. All simulations were performed in Matlab with Simulink. The channel model used for all simulations is based on measurements of 399 m of multimode fiber [12]. The unequalized pulse response at 10 Gb/s ($T = 100$ ps) is plotted in Fig. 4(a). Note that this is a much more stressful channel than was simulated in [4], making pattern-dependent jitter particularly important.

To model the effect of bandwidth-limited transmitter and receiver circuitry, first-order lowpass filters with -3 -dB cutoff frequencies of 8 GHz were included at either end of the link. Additive white Gaussian noise was introduced with a signal-to-noise ratio of 30 dB at the equalizer input. The resulting unequalized binary eye pattern is shown in Fig. 4(b). All simulations were performed using a $2^{31} - 1$ pseudorandom binary data sequence. The 10^{-15} BER contours for equalized eye patterns are calculated from the known channel response, noise and jitter statistics, assuming uncoded random data.

The simulated CDR uses an Alexander phase detector in a data-referenced second-order phase-locked loop to recover the clock. The voltage-controlled oscillator (VCO) gain is 200 MHz/V, the gain in the integral path is 10^{-8} , and the gain in the proportional path is 0.2. Random jitter in the transmitter clock was also included in the simulations with a bounded gaussian distribution having 0.01 UI rms and 0.08 UI peak-to-peak amplitude. The adaptation loops were data-driven (blind) using the data recovered by the CDR as the equalizer’s “desired” output.

A. Baud-Rate Equalization

In this section, a 5-tap baud-rate ($\tau = T$) equalizer is assumed. Assuming random data, the tap outputs \vec{u} are uncorrelated so there is no risk of equalizer coefficient drift after convergence. Therefore, ζ may be omitted from the adaptation algorithm’s objective function. This is accomplished by setting $a_3 = 0$ in (9). For sign–sign LMS adaptation, $a_1 = 1$ and $a_2 = 0$ in (9). For the signed jitter-reducing adaptation simulations $a_1 = a_2 = 1$. In all cases, the adaptation constant was set to $\mu = 1.5 \cdot 10^{-4}$ and tap 2 was the “main” tap. The value of μ was chosen to provide convergence within approximately 10^5 bit periods, or 0.01 ms at 10 Gb/s. This is fast enough to track

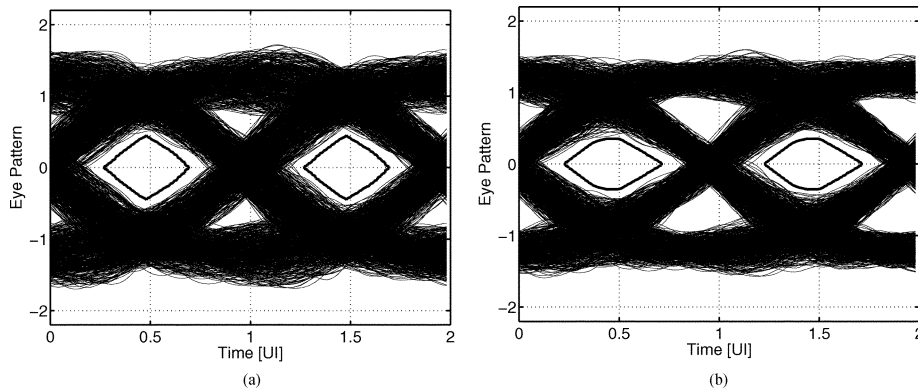


Fig. 6. Eye diagrams and $\text{BER} = 10^{-15}$ contours at the output of a 5-tap baud-rate equalizer adapted using: (a) the traditional sign–sign LMS algorithm, and (b) the signed jitter-reducing adaptation algorithm.

variations in multimode fiber channels, generally expected to occur over tens of milliseconds [13].

The equalized pulse responses after convergence are shown in Fig. 5 for both the sign–sign LMS adaptation and signed jitter-reducing adaptation algorithms. The markers in Fig. 5 denote the locations where the pulse response is being sampled by the CDR. The LMS algorithm is more effective at canceling the first pre- and post-cursor ISI terms. The LMS algorithm also has a slightly larger main pulse amplitude. As a result, the LMS algorithm has a greater vertical eye height, as shown in Fig. 6(a). However, the signed jitter-reducing adaptation algorithm introduces less ISI *between* samples (particularly precursor), which translates into less pattern-dependent jitter and less noise enhancement. This explains the slightly larger horizontal eye opening observed in Fig. 6(b).

The simulation results for a baud-rate equalizer predict marginally better timing performance using signed jitter-reducing adaptation, obtained at the expense of decreased noise margin (vertical eye opening). Results from the next section will show that the improvement is more dramatic when adapting a fractionally spaced equalizer.

B. Fractionally Spaced Equalization

Fractionally spaced equalization has been proposed for 10 Gb/s fiber links in, for instance, [5], [14]. Part of the motivation for its use has been that the performance of a fractionally spaced equalizer is relatively independent of sampling phase [9].² However, for data rates exceeding 1 Gb/s, practical equalizer adaptation algorithms are too slow to track jitter on the recovered clock. Therefore, as the simulations in this section will show, timing margin is actually *degraded* by using fractional tap-spacing unless an appropriate adaptation algorithm is employed that explicitly includes low jitter as part of its optimization criteria.

In this section, a 10-tap $T/2$ -spaced equalizer is used, with the second tap serving as the “main” one. Simulations indicated that leakage in the coefficient update integrator was required (i.e., $a_3 \neq 0$) to prevent excessive tap weight drift due to the

²Another benefit of fractional tap-spacing is that it implements a matched filter. However, in binary NRZ links, the approximate matched filtering provided for free by the receiver’s bandwidth-limited front end is generally sufficient.

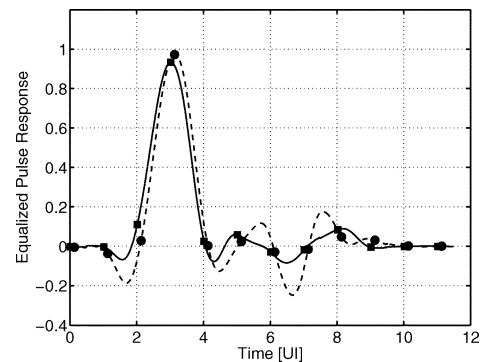


Fig. 7. Equalized pulse responses with a 10-tap $T/2$ -spaced equalizer adapted using the traditional sign–sign LMS algorithm (dashed line, circular markers) and the signed jitter-reducing adaptation algorithm (solid line, square markers).

correlation between successive tap signals. The adaptation constants used were $\mu = 1.5 \cdot 10^{-5}$, $a_1 = 1$, and $a_3 = 0.1$. For traditional sign–sign LMS adaptation $a_2 = 0$, and for the signed jitter-reducing adaptation algorithm, $a_2 = 1$. The adaptation rate was slower than with baud-rate tap-spacing, but still fast enough to track typical channel variations.

The equalized pulse responses are plotted in Fig. 7; again, the sign–sign LMS algorithm provides better ISI cancellation at the sampling instants (markers), but less ISI cancellation *between* samples. The increase in recovered clock jitter seriously compromises the eye opening at a BER of 10^{-15} , as shown in Fig. 8(a). In fact, fractionally spaced equalization results in a much narrower eye opening than baud-rate equalization [Fig. 6(a)] when a simple LMS criteria is used for the adaptation. In general, whenever MSE at the sampling instants is used as the only criteria for optimization of equalizer tap weights, overall eye quality (particularly timing margin) may be sacrificed to obtain what are often only small improvements in MSE. For instance, simulations of a minimum MSE equalizer (which is slightly different from that obtained by LMS adaptation due to the nonzero leakage term, a_3) demonstrated an even poorer eye quality and BER at the equalizer output.

The jitter-reducing adaptation algorithm compromises between maximizing the MSE at the center of the eye and at zero-crossings, thereby making the eye wider and decreasing jitter in the recovered clock. As a result, a fractionally spaced equalizer demonstrates both improved noise margin *and* timing

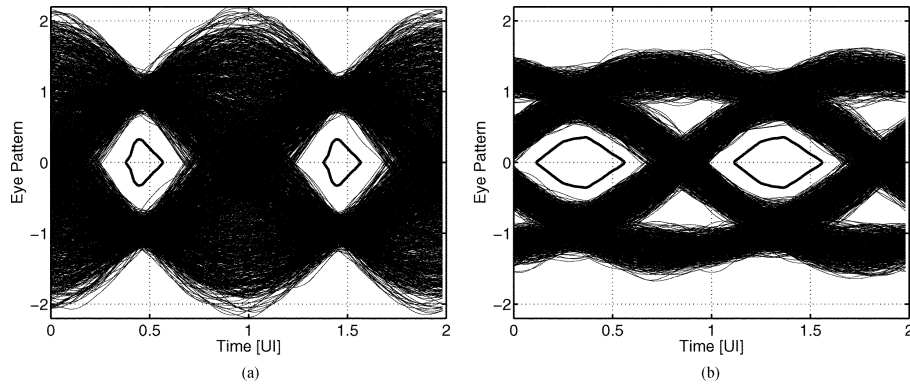


Fig. 8. Eye diagrams and $\text{BER} = 10^{-15}$ contours at the output of a 10-tap $T/2$ -spaced equalizer adapted using: (a) the traditional sign–sign LMS algorithm, and (b) the signed jitter-reducing adaptation algorithm.

TABLE I

SUMMARY OF SIMULATION RESULTS FOR A 5-TAP BAUD-RATE EQUALIZER AND A 10-TAP $T/2$ -SPACED EQUALIZER USING THE SIGN-SIGN LMS (SS-LMS) AND JITTER-REDUCING (J-R) ADAPTATION ALGORITHMS. (EYE OPENINGS MEASURED AT A BER OF 10^{-15})

	Baud-Rate		Fractionally-Spaced	
	SS-LMS	J-R	SS-LMS	J-R
Noise Amplification [dB]	2.76	2.04	4.39	1.98
Vert. Eye Opening	0.90	0.70	0.66	0.73
Horiz. Eye Opening [UI]	0.42	0.48	0.19	0.45
Rx Clock Jitter [mUI _{rms}]	14	12	22	15

margin. In this case, the improvement over traditional sign–sign LMS adaptation is 11% in vertical eye opening and 137% in horizontal eye opening at a BER of 10^{-15} . The results for both the baud-rate and fractionally spaced equalizer simulations are summarized in Table I.

IV. CONCLUSION

For binary communication links over 1 Gb/s, timing margin at the receiver is often more critical than vertical noise margin. Jitter decreases timing margin at the receiver and hinders the recovery of a low-jitter clock. However, high data-rate channels are often equalized using the LMS or related algorithms which are designed to optimize only the vertical eye opening. In this brief, the mean squared error at both the center of the received eye and at transitions in the received eye are simultaneously minimized using a weighted objective function.

A hardware-efficient implementation of this adaptation algorithm has been also been described. This signed jitter-reducing adaptation algorithm uses 1-bit (signed) versions of state and error signals similar to sign–sign LMS adaptation and can be efficiently combined with binary phase detection in an integrated receiver.

Behavioral simulations verified the technique on a 10-Gb/s optical fiber link. The simulations predict a marginal improvement in timing performance when signed jitter-reducing adaptation is compared with traditional sign–sign LMS adaptation in a baud-rate equalizer. In a fractionally spaced equalizer, signed jitter-reducing adaptation provides dramatic improvements in both vertical and horizontal eye opening. In fact, timing margin can actually be *degraded* by using fractional tap-spacing unless

an appropriate adaptation algorithm (such as the one described here) is employed.

REFERENCES

- [1] J. Buckwalter and A. Hajimiri, "A 10 Gb/s data-dependent jitter equalizer," in *Proc. Custom Integr. Circuits Conf.*, Sep. 2004, pp. 39–42.
- [2] V. Stojanovic, A. Amirkhany, and M. Horowitz, "Optimal linear precoding with theoretical and practical data rates in high-speed serial-link backplane communication," in *Proc. IEEE Int. Conf. Commun.*, Jun. 2004, pp. 2799–2806.
- [3] B. Brunn, Edge-equalized NRZ HP Labs, Palo Alto, CA, 2004 [Online]. Available: http://www.ieee802.org/3/ap/public/jul04/brunn_01_0704.pdf
- [4] A. C. Carusone, "Jitter equalization for binary baseband communication," in *Proc. IEEE Int. Symp. Circuits Syst.*, May 2005, pp. 936–939.
- [5] H. Wu, J. A. Tierno, P. Pepejugoski, J. Schaub, S. Gowda, J. A. Kash, and A. Hajimiri, "Integrated transversal equalizers in high-speed fiber-optic systems," *IEEE J. Solid-State Circuits*, vol. 38, no. 12, pp. 2131–2137, Dec. 2003.
- [6] J. Sewter and A. C. Carusone, "A CMOS finite impulse response filter with a crossover traveling wave topology for equalization up to 30 Gb/s," *IEEE J. Solid-State Circuits*, vol. 41, no. 6, pp. 909–917, Apr. 2006.
- [7] J. D. H. Alexander, "Clock recovery from random binary data," *Electron. Lett.*, pp. 541–542, Oct. 1975.
- [8] J. Rogers and J. Long, "A 10-Gb/s CDR/DEMUX with LC delay line VCO 0.18- μm CMOS," *IEEE J. Solid-State Circuits*, vol. 37, no. 12, pp. 1781–1789, Dec. 2002.
- [9] G. Ungerboeck, "Fractional tap-spacing equalizer and consequences for clock recovery in data modems," *IEEE Trans. Commun.*, vol. 24, no. 8, pp. 856–864, Aug. 1976.
- [10] R. D. Gitlin, H. C. Meadors, and S. B. Weinstein, "An algorithm for the stable operation of a digitally implemented fractionally spaced adaptive equalizer," in *Proc. IEEE Int. Conf. Acoust., Speech, Signal Process.*, May 1982, pp. 1379–1382.
- [11] J. E. Jaussi, G. Balamurugan, D. R. Johnson, B. K. Casper, A. Martin, J. T. Kennedy, N. Shanbhag, and R. Mooney, "An 8 Gb/s source-synchronous I/O link with adaptive receiver equalization, offset cancellation and clock deskew," in *Proc. IEEE Int. Solid-State Circuits Conf.*, Feb. 2004, pp. 246–247.
- [12] L. Aronson and L. Buckman, HP Labs ROFL/OFL fiber measurements HP Labs, Palo Alto, CA, 1997 [Online]. Available: <http://grouper.ieee.org/groups/802/3/z/mbi>
- [13] J. Dallesasse, Modification of comprehensive stressed receiver sensitivity and overload test for verification of equalizer adaptation time Emcore Corporation, Somerset, NJ, 2005 [Online]. Available: http://ieee802.org/3/aaq/public/may05/dallesasse_1_0505.pdf
- [14] S. Pavan and S. Shivappa, "Nonidealities in traveling wave and transversal FIR filters operating at microwave frequencies," *IEEE Trans. Circuits Syst. I, Reg. Papers*, vol. 53, no. 1, pp. 177–192, Jan. 2006.